

See discussions, stats, and author profiles for this publication at: <https://www.researchgate.net/publication/221971992>

Single and Double Core-Hole Ionization Energies in Molecules

ARTICLE *in* THE JOURNAL OF PHYSICAL CHEMISTRY A · MARCH 2012

Impact Factor: 2.69 · DOI: 10.1021/jp211741e · Source: PubMed

CITATIONS

16

READS

35

1 AUTHOR:



Thomas Darrah Thomas

Oregon State University

215 PUBLICATIONS 5,546 CITATIONS

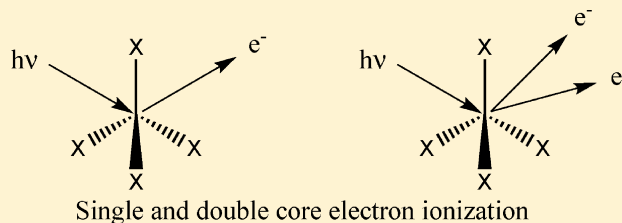
SEE PROFILE

Single and Double Core-Hole Ionization Energies in Molecules

T. Darrah Thomas*

Department of Chemistry, Oregon State University, Corvallis, Oregon 97331, United States

ABSTRACT: The recently demonstrated ability to measure double-hole core-ionization energies in first-row elements has led to a renewed interest in the use of such energies to investigate the effects of initial-state charge distribution and final-state charge rearrangement on the energies of chemical processes that involve addition of charge to a molecule. With theoretical calculations for the molecules $\text{CH}_{4-n}\text{X}_n$, $\text{X} = \text{F}, \text{Cl}$, and for $\text{C}(\text{CH}_3)_4$ as a basis, the relationships between one-hole and two-hole ionization energies, on one hand, and initial-state and final-state effects, on the other, are reviewed. It is shown that higher-order corrections to the traditionally used relationships are quantitatively significant but do not lead to qualitatively different conclusions. The role of the Wagner plot as a way to display the relationships among the various quantities of interest is discussed, and a generalized Wagner plot for displaying two-site double-hole ionization energies is presented. Some possible applications of measurements of double-hole ionization energies to the investigation of molecular conformation and molecular fragmentation are discussed.



INTRODUCTION

Many chemical phenomena depend on the ability of a molecule to accept or give up charge at a particular atom in the molecule. Among these are core ionization (removal of one or more inner-shell electrons from an atom), protonation or Brønsted basicity (addition of a proton at a particular site), deprotonation or Brønsted acidity (removal of a proton from a particular site), and electrophilic reactivity (involving formation of a transition state with charge localized at a particular site). As chemists, we are typically interested in how the energies for these processes differ between molecules with different structures or compositions. To a good approximation, these relative energies depend on two factors: the differences in the charge distributions in the initial molecules, which affect the potential energy at the site of the added charge, and the polarizabilities of the molecules, which reflect the relative abilities of the molecules to respond to the added charge.

Determining the contributions of these two effects can enhance the understanding of these various chemical phenomena, and as a result, a number of techniques, both experimental and theoretical, have been developed for this purpose. Among these, an important approach is the comparison of single-hole and double-hole core-ionization energies. Typically, the single-hole ionization energies have been measured by photoelectron spectroscopy and the double-hole ionization energies by core–core–core Auger spectroscopy, and extensive use of this technique has been made to investigate systems of chemical interest.^{1–5} The disadvantage of this approach is that it is restricted to elements of the second row and higher, as no core–core–core transitions are possible for first-row elements (with the possible exception of fluorine⁴). Recently, however, it has become possible to measure double-hole core-ionization energies directly,^{6–9} opening up the possibility of investigating the rich chemistries of carbon,

nitrogen, and oxygen. These studies have arisen not only because of newly available experimental capabilities, but also in response to a number of theoretical works on double-hole ionization energies. In these works, particular emphasis has been placed on two-site double-hole ionization with discussion of how it might be observed and what new insights might be gained from the two-site double-hole ionization energies.^{10–13}

These recent works have not only opened up new opportunities but also produced some new ways of looking at old problems. It is useful, therefore, to consider the relationships between some of these new perspectives and the older ones. In addition, it is important to explore some of the limitations of the models that have been used to describe these phenomena. With these goals in mind, I report herein the results of theoretical calculations on the one- and two-hole carbon 1s core-ionization energies of the fluorinated and chlorinated methanes ($\text{CH}_{4-n}\text{X}_n$, $\text{X} = \text{F}, \text{Cl}$) and the central carbon in 2,2-dimethylpropane, $\text{C}(\text{CH}_3)_4$. These species were chosen to provide one example in which the effects of polarizability are quite small (the fluoromethanes), one in which these effects are significant (the chloromethanes), and one in which the relaxation effect is larger than the initial-state effect (2,2-dimethylpropane). The results are compared with those obtained from experimental measurements combined with theory, and good agreement is found provided that due attention is paid to higher-order corrections.

There have been many discussions of the relationships between one- and two-hole energies^{14–18} and between these and other chemical properties, such as acidity,^{19–22} basicity,^{19,23–26} and reactivity.^{26,27} The basic principles of all of these

Received: December 6, 2011

Revised: March 23, 2012

Published: March 23, 2012

approaches can be understood in terms of a simple model. Consider the energy, $E(q)$, of a molecule as a function of charge q added at a specific site, which can be written as

$$E(q) - E(0) = q \left(\frac{dE}{dq} \right)_0 + (q^2/2) \left(\frac{d^2E}{dq^2} \right)_0 + \dots \quad (1)$$

where the derivatives are evaluated for the neutral molecule.²⁸ For deprotonation (acidity), the first derivative is equal to the potential energy of the proton, V .²² For electrons, the first derivative has been identified as the Koopmans theorem ionization energy (equal to $-\epsilon$, where ϵ is the orbital energy of a Hartree–Fock calculation).^{17,18,29} In either case, this term depends only on the wave functions of the neutral molecule and can be identified as an initial-state effect. The second (and higher) terms involve changes to the molecular wave functions because of the added charge and can, therefore, be interpreted as the contribution to the energy from charge rearrangement, that is, the relaxation energy, R .

To simplify this expression, one can replace $(dE/dq)_0$ with V and $(d^2E/dq^2)_0/2$ with $-R$, which reflects the modification of the potential energy of a unit positive charge by the polarization of the molecule that is induced by the added charge. Then

$$\Delta E(q) = E(q) - E(0) = qV - q^2R + \dots \quad (2)$$

If one sets $q = 1$, then eq 2 gives the one-hole ionization energy, I_1 , and the enthalpy of protonation (basicity), P . With $q = -1$, eq 2 gives the enthalpy of deprotonation (acidity), A . With $q = 2$, one has the two-hole ionization energy, I_2 , but in this case, one must also include the Coulomb interaction energy, V_C , between the two holes. These different energies differ from one another in absolute amount because the processes that give rise to them are quite different. However, if one is concerned with the effects of changes in the molecule that are remote from the site of interest, it is reasonable to assume that the changes in these energies due to changes in the molecular composition will be approximately independent of the process. Then, one has

$$\Delta I_1(0) = \Delta V - \Delta R \quad (3)$$

$$\Delta P(0) = \Delta V - \Delta R \quad (4)$$

$$\Delta A(0) = -\Delta V - \Delta R \quad (5)$$

$$\Delta I_2(0) = 2\Delta V - 4\Delta R + \Delta V_C \approx 2\Delta V - 4\Delta R \quad (6)$$

where the right-hand version of eq 6 takes into account that V_C for two holes in the same atomic core is an atomic property that is assumed to be independent of the molecular composition or structure.³⁰ In these expressions, the arguments of 0 indicate that the properties represent those of the neutral molecule. An expression can also be written for the second ionization energy, $I_1(+1)$, which is the difference between the two-hole and one-hole ionization energies. A similar expression exists (with opposite sign) for the core–core–core Auger kinetic energy, K_A , which is equal to the difference in energy between a deep-lying one-hole core state and a less deep two-hole core state. In addition, one has the Auger parameter α' , which is defined as the sum of the Auger energy and the one-hole ionization energy.² Thus

$$\begin{aligned} \Delta I_1(+1) &\equiv \Delta I_2(0) - \Delta I_1(0) \\ &= \Delta V - 3\Delta R \\ &= \Delta I_1(0) - 2\Delta R \end{aligned} \quad (7)$$

$$\begin{aligned} \Delta K_A &\equiv -[\Delta I_2(0) - \Delta I_1(0)] \\ &= -\Delta V + 3\Delta R \\ &= -\Delta I_1(0) + 2\Delta R \end{aligned} \quad (8)$$

$$\begin{aligned} \Delta \alpha'(0) &\equiv \Delta K_A + \Delta I_1(0) \\ &\equiv \Delta I_1(0) - \Delta I_1(+1) \\ &= 2\Delta R \end{aligned} \quad (9)$$

where the minus sign in the first line of eq 8 reflects the fact that the Auger kinetic energy is the negative of the transition energy. Extensive use of the Auger parameter has been made as a tool for both characterizing solids¹ and determining relaxation energies in gas-phase molecules.^{3–5} In addition, eqs 3 and 5 have been used in conjunction with measured gas-phase acidities and core-ionization energies through the relationships $\Delta R = -[\Delta I_1(0) + \Delta A(0)]/2$ and $\Delta V = [\Delta I_1(0) - \Delta A(0)]/2$.^{19–22} Comparison of eq 3 with eq 4 indicates that core-ionization energies should be directly correlated with enthalpies of protonation, and such correlations are known for a number of systems.^{19,23–26}

■ THEORETICAL CALCULATIONS

To gain insight into the relationships outlined in the preceding section and their limitations, I calculated theoretically the energies for the fluorinated and chlorinated methanes ($\text{CH}_{4-n}\text{X}_n$, $\text{X} = \text{F}, \text{Cl}$) and for $\text{C}(\text{CH}_3)_4$ having zero, one, and two holes in the 1s shell of the central carbon atom. These calculations were performed using the Gaussian 09 programs.³¹ Three sets of calculations were done. For two of these, the core holes were modeled using an effective core potential, scaled to represent the correct number of holes. The basis set for these calculations was a triple- ζ basis set with polarization functions, which has been found to be effective in calculation of carbon 1s ionization energies; details of this basis set and the effective core potential are given elsewhere.³² For the chlorine atoms, the 6-311G(2d) basis set was used. For the first set of calculations, the B3LYP method was used. The optimized geometry for the neutral molecule was used for all calculations to focus on the parts of the energy shifts that are due to electronic effects rather than those that are due to geometric effects. The second set of calculations used the MP4SDQ method at the B3LYP geometry. Previous experience calculating the carbon 1s ionization energies of hydrocarbons has shown that this approach gives better results than the B3LYP method, without a great expense in calculation time.³²

The disadvantage of the methods just described is that they can give results only for three points: for zero, one, and two holes in the carbon 1s shell. The analysis is thus limited to only the linear and quadratic terms in eq 1. To go beyond this limitation, I used the equivalent-cores approach [with the 6-311g(d,p) basis set and the B3LYP method]. In this approximation, singly core-ionized CH_4 is replaced by NH_4^+ and doubly core-ionized CH_4 is replaced by OH_4^{2+} . The advantage of this method is that it can be extended to the hypothetical species having an extra electron in the carbon 1s shell (BH_4^-) or three holes in the carbon 1s shell (FH_4^{3+}). Calculation of the energies

for these additional species provides information on the higher terms that have been omitted from eq 1.

Closely related to the equivalent-cores approach is the technique of varying the effective charge on the carbon atom in small steps. This can be done by including a set of additional charges, q , very close to the carbon atom. For this purpose, I used a set of four charges located 0.01 Å from the carbon atom in the directions of the ligands and performed calculations for $q = \pm 0.0025, \pm 0.005, \pm 0.01, \pm 0.02$, and ± 0.03 . The energies obtained from the calculations are corrected for the self-energy of the assembly of additional charges and for their interaction energy with the carbon nucleus. This method makes it possible to investigate in some detail the behavior of eq 1 for an additional charge close to zero.

None of the methods outlined above gives absolute energies for the ionized species. However, they do give the energies of one compound relative to another. As a consequence, it is necessary first to take the difference between the calculated energy for the ion of interest and that of a suitable reference compound in the same state of ionization. The reference compound used here is methane, and accordingly, all energies were calculated relative to that of methane in the appropriate state of ionization. Furthermore, from a chemical point of view, one is interested in the shifts of ionization energies relative to those of methane. Consequently, all energies are presented relative to that for methane. Thus, for example, $\Delta I_2(0, \text{CF}_4)$, the two-hole energy of CF_4 relative to CH_4 , is expressed as

$$\Delta I_2(0, \text{CF}_4) = E(2, \text{CF}_4) - E(2, \text{CH}_4) - E(0, \text{CF}_4) + E(0, \text{CH}_4)$$

where $E(n, \text{CX}_4)$ is the calculated energy for the indicated species.

The results of these calculations are reported in Table 1. Also included in this table are values derived from experimental measurements of the carbon 1s ionization energies.³³ For the ionization energies, shown as the first set of results in the table, there is good agreement between the theoretically calculated shifts and the experimental values, although the theoretical predictions tend to overestimate the shifts. There is good agreement among the three theoretical methods, as can be seen in Figure 1, where the calculated values for the second core-ionization energy, $I_1(+1)$, are plotted against the first core-ionization energy, $I_1(0)$. The details of this figure are discussed in the following section.

From Table 1, one can see that the theoretical results for ΔR , shown as the second group of results, are in qualitative agreement with those derived from experimental measurements.³⁴ For the fluoromethanes, all of the approaches agree that relaxation makes a minor contribution to the shifts. For chlorine, they all show that significant relaxation is associated with chlorine, increasing with the number of chlorine atoms. For 2,2-dimethylpropane, they show that the small shift in ionization energy results from the near-cancellation of a large value of ΔV by an even larger value of ΔR .³⁵ In detail, however, there are disagreements between the experimentally based results and those derived from the theoretical approach used here. In particular, the experimentally derived relaxation-energy shifts for fluorine are negative, implying that fluorine is less polarizable than hydrogen, whereas the theoretically based results show that these shifts are slightly positive. For the chloromethanes and for 2,2-dimethylpropane, the relaxation-energy shifts from theory are noticeably greater than those

Table 1. Vertical Carbon 1s Ionization Energies, Relaxation Energies, and Initial-State Potential Energies for Fluorinated and Chlorinated Methanes and for 2,2-Dimethylpropane^a

	expt ³³	B3LYP	MP4SDQ	equivalent cores
Ionization Energies, ΔI				
CH_3F	2.713	2.811	3.036	2.671
CH_2F_2	5.502	5.680	5.852	5.449
CHF_3	8.315	8.534	8.782	8.351
CF_4	11.054	11.246	11.568	11.299
CH_3Cl	1.586	1.751	1.643	1.722
CH_2Cl_2	2.966	3.283	3.197	3.221
CHCl_3	4.316	4.574	4.449	4.577
CCl_4	5.486	5.896	5.838	5.842
$\text{C}(\text{CH}_3)_4$	-0.187	-0.296	-0.134	-0.289
Relaxation Energies, ΔR^b				
CH_3F	-0.183	0.099	0.233	0.066
CH_2F_2	-0.450	0.145	0.189	0.093
CHF_3	-0.750	0.162	0.218	0.133
CF_4	-1.032	0.171	0.212	0.233
CH_3Cl	0.542	0.865	0.771	0.860
CH_2Cl_2	1.037	1.493	1.434	1.505
CHCl_3	1.392	1.973	1.917	2.051
CCl_4	1.857	2.445	2.456	2.551
$\text{C}(\text{CH}_3)_4$	1.103	1.648	1.642	1.680
Initial-State Energies, ΔV^c				
CH_3F	2.530	2.911	3.269	2.737
CH_2F_2	5.053	5.825	6.041	5.542
CHF_3	7.565	8.696	9.000	8.484
CF_4	10.022	11.417	11.780	11.532
CH_3Cl	2.128	2.616	2.415	2.583
CH_2Cl_2	4.003	4.775	4.631	4.727
CHCl_3	5.708	6.547	6.367	6.628
CCl_4	7.343	8.340	8.294	8.393
$\text{C}(\text{CH}_3)_4$	0.916	1.352	1.508	1.392

^aValues are in electronvolts and are given relative to those for methane. ^bValues of ΔR in the experimental column were calculated from the experimental ionization energies and values of ΔV obtained using the extended Koopmans theorem:³⁶ $\Delta R = \Delta V - \Delta I$. ^cValues of ΔV in the experimental column were calculated theoretically using the extended Koopmans theorem.³⁶

derived from experiment. These areas of disagreement are discussed in a subsequent section, where it is shown that they arise from the omission of the higher-order terms in eq 1.

The values of ΔV , seen in the third group of Table 1, are consistent with chemical experience. The three substituents, F, Cl, and CH_3 , are all more electronegative than the hydrogen atoms that they replace, and as a consequence, all of the values of ΔV are positive and increase with the number of substituents. However, the values obtained from the theoretical calculations discussed here are all systematically greater than those obtained from the extended Koopmans theorem proposed by Børve and Thomas.^{33,36} This point is discussed in more detail in the section Higher-Order Effects.

■ WAGNER PLOTS AND THE AUGER PARAMETER

In considering the core-ionization and Auger energies for solids, Wagner developed the concept of the Auger parameter,¹⁶ α , which he defined as the difference between the measured Auger kinetic energy, K_A , and the kinetic energy of a photoelectron, K_e . He showed that this difference is related to the polarizability of the environment of the ionized atom and

that shifts in the Auger parameter, $\Delta\alpha$, between one sample and another were equal to twice the relaxation energy, as seen in eq 9.

Wagner's original definition was convenient for his immediate concern, which was characterizing solids, especially nonconducting solids. Because the Auger parameter was defined as the difference between two kinetic energies measured in the same sample, any effects of charging or choice of reference level cancel. A version of this parameter that is now more commonly used is α' , which includes the energy of the photon, $h\nu$.^{2,37} Thus

$$\alpha' = K_A - K_e + h\nu = K_A + I_1(0)$$

where $I_1(0)$ is the ionization energy for the appropriate core level.

Wagner also introduced what he called the "chemical-state plot", in which the Auger kinetic energy is plotted against the photoelectron kinetic energy.³⁸ Now known as "Wagner plots", the present-day version involves plotting the Auger kinetic energy against the core-hole ionization energy, but for consistency with Wagner's original idea, the values are plotted with the ionization energy increasing from right to left.³⁷ Wagner plots provide a convenient way to summarize the relationships between one-hole ionization energies, Auger energies, relaxation energies, and initial-state effects for related series of compounds. Because of the potential usefulness of such plots, a wealth of data has been accumulated on a variety of substances and is available in the form of Wagner plots.^{37,39}

Although it does not directly involve Auger energies, Figure 1 is a Wagner plot. The abscissa shows the ionization energy

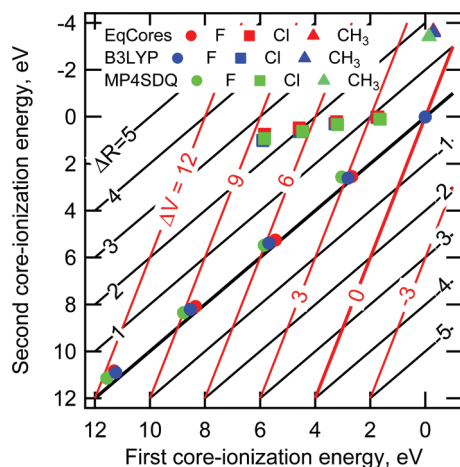


Figure 1. Calculated second carbon 1s ionization energy for fluorinated and chlorinated methanes and for 2,2-dimethylpropane plotted against the first carbon 1s ionization energy. The black lines indicate loci of constant ΔR , and the red lines indicate loci of constant ΔV .

(relative to that of methane) for a single hole in the carbon 1s shell, plotted, as in a Wagner plot, from right to left. The ordinate shows the second carbon 1s ionization energy (again, relative to that of methane), which is equal to $\Delta I_2(0) - \Delta I_1(0)$, plotted with the value increasing from top to bottom. As established in the following discussion, this quantity is the same as that plotted in a standard Wagner plot.

The Auger kinetic energy is equal to the difference between the final-state two-hole energy, $I_2(0)$, and the energy of the original core hole, $I_1'(0)$ (where the prime indicates that the

initial one-hole state is in a different shell from the final two-hole state). Thus, $K_A = I_1'(0) - I_2(0)$. The second core-hole ionization energy is given by $I_1(+1) = I_2(0) - I_1(0)$. The two expressions differ in that one involves the ionization energy of a deep core hole, $I_1'(0)$, and the other the ionization energy of a less deep hole, $I_1(0)$. The interest here, however, is in shifts in these energies arising from changes in the composition of the molecules, and, in this case, a reasonable approximation is that these are the same for different core levels.⁴⁰ Thus, $\Delta I_1(0) \approx \Delta I_1'(0)$, and in consequence, $\Delta I_1(+1) \approx -\Delta K_A$. With this relationship in mind, one can see that the plot shown in Figure 1 is essentially a Wagner plot, but one involving relative rather than absolute energies. It differs from the usual Wagner plot only by additive shifts on the two axes.

The Wagner plot provides a convenient way to summarize data on two-hole ionization energies, as well as to visualize the initial-state and relaxation effects. From either eq 7 or eq 9, one can see that lines with slopes of +1 are loci of constant ΔR , with intercepts on the ordinate equal to $-2\Delta R$. A series of these lines is indicated in black in Figure 1, where the heaviest line indicates $\Delta R = 0$, that is, no difference from the relaxation energy of the reference compound. The points for the fluorinated methanes fall close to this line, consistent with the small values of ΔR listed in Table 1. By contrast, the points for the chloromethanes fall above the $\Delta R = 0$ line, consistent with the large relaxation effects associated with chlorine as a substituent.

Solving eqs 3 and 6 for ΔV and using eq 7, one obtains the relationship $\Delta I_1(+1) = 3\Delta I_1(0) - 2\Delta V$. Thus, loci of constant ΔV have slopes of 3 and intercepts of $-2\Delta V$. A series of such loci are shown in red in Figure 1, and from these, one can easily see the role of the initial-state effect in the ionization energies of the halomethanes.

Figure 2 shows a Wagner plot of recently measured results for methane,⁷ ethyne,⁹ and carbon dioxide⁸ (red squares). In this graph the absolute values of the ionization energies are used rather than shifts. Also shown here are results of theoretical calculations for ethane, ethene, ethyne, carbon monoxide, and carbon dioxide¹¹ (shown as blue circles) and for

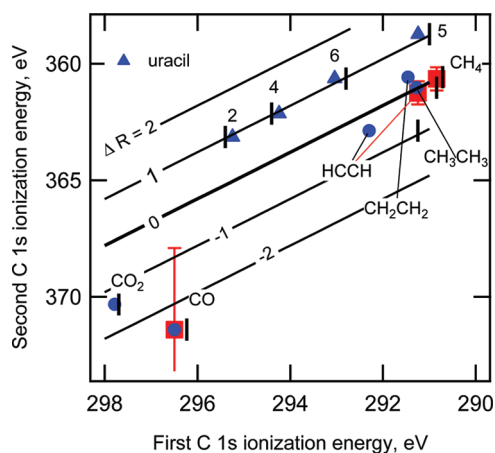


Figure 2. Wagner plot for carbon 1s ionization. The red squares show experimental measurements for methane,⁷ ethyne,⁹ and carbon monoxide.⁸ The blue circles show theoretical predictions from ref 11, and the blue triangles show theoretical predictions for uracil.¹² The horizontal positions of the small black vertical lines indicate the experimental one-hole ionization energies.⁴¹ The diagonal black lines indicate loci of constant ΔR .

the carbon atoms in uracil¹² (blue triangles). The theoretical calculations were shifted to align with the experimental point for carbon monoxide. The shifts were 0.14 eV for the single-hole ionization energies and 3.34 eV for the double-hole energies. The short vertical black lines indicate the measured carbon 1s single-hole vertical ionization energies,⁴¹ which show that, for the most part, there is reasonable agreement between the theoretical and experimental results. As in Figure 1, the diagonal lines show loci of constant ΔR . The heavy black line is drawn through the points for methane and ethane, which provide a reference point.

First to be noticed in Figure 2 is the negative relaxation contribution to the methane–carbon monoxide shift of more than 2 eV, implying that carbon monoxide is significantly less polarizable than methane. This experimental result is in accord with the calculations of Tashiro et al.,¹¹ who, although they do not give results for methane, reported a relaxation contribution to the ethane–carbon monoxide ionization-energy shift of -3.2 eV.

The four points for the carbon atoms in uracil fall almost exactly on a line of constant relaxation energy. Moreover, the position of these points is above the reference line for $\Delta R = 0$, indicating that the relaxation energy associated with these carbons is greater than that for methane and ethane. This observation is in keeping with experience that relaxation increases with the size of the molecule. A plot similar to this was presented by Takahashi et al.,¹² who noted that the slope was close to 1. They also concluded that the relaxation energy for all of these carbon atoms was about the same.

Recently, it has become possible to measure the ionization energies to remove two electrons not only from the same atom (one-site), but also from different atoms in the same molecule (two-site).⁸ Along with the experimental demonstration of this ability, a number of theoretical works have aimed at illustrating the kinds of information that can be obtained about a variety of molecules from such measurements.^{10–12} Takahashi et al.¹² displayed the results of their calculations by plotting, effectively, the second core-ionization energy versus the first, as in the Wagner plot. There are two problems with this approach. In the ordinary Wagner plot, one is dealing with two holes on the same atom. Thus, all of the two-hole ionization energies are affected by nearly the same value of the Coulomb interaction energy, whereas in two-site ionization there are different values of this energy, depending on the distance between the two sites. The second problem is that such a plot has two points for each different two-hole site, each one representing a different choice of which atom is ionized first. For both of these reasons, it is hard to visualize what essential information can be gleaned from such a plot.

To develop a modification of the Wagner plot suitable for including two-site ionization, consider an expansion of eq 1 to include the possibility of ionization from two sites, i and j . This becomes

$$E(q_i, q_j) - E(0) = q_i \left(\frac{dE}{dq_i} \right)_0 + q_j \left(\frac{dE}{dq_j} \right)_0 + (q_i^2/2) \left(\frac{d^2E}{dq_i^2} \right)_0 + (q_j^2/2) \left(\frac{d^2E}{dq_j^2} \right)_0 + q_i \left(\frac{d^2E}{dq_i dq_j} \right)_0 + V_{ij} \dots \quad (10)$$

where V_{ij} is the Coulombic interaction energy between the two holes. Focusing on the case of interest, $q_i = q_j = 1$, and using the definitions of V and R given above, one obtains

$$I_{2,ij} \equiv E(1, 1) - E(0) = V_i + V_j - R_i - R_j - R_{ij} + V_{ij} \dots \quad (11)$$

where $R_{ij} = -d^2E/(dq_i dq_j)$. The term R_{ij} arises because the environment with which each hole interacts is modified by the presence of the other hole. This quantity is referred to as “generalized relaxation energy” or, if the two holes are on different sites, as an “interatomic generalized relaxation energy”.^{11,12} Using eq 3, eq 11 can also be written in terms of the one-hole ionization energies, $I_{1,i}$ and $I_{1,j}$, to give¹¹

$$I_{2,ij} \equiv E(1, 1) - E(0) = I_{1,i} + I_{1,j} - R_{ij} + V_{ij} \dots \quad (12)$$

For two-site ionization, $V_{ij} = 1/r_{ij}$ (in atomic units), where r_{ij} is the distance between the two ionized atoms. This distance can be known either from measurements or from molecular structure calculations. It is then convenient to move V_{ij} to the left-hand side of eq 12 and to define a modified two-hole ionization energy, $I_{2,ij}^* = I_{2,ij} - V_{ij}$. Then

$$I_{2,ij}^* = I_{1,i} + I_{1,j} - R_{ij} \dots \quad (13)$$

Equation 13 suggests that a useful way to display the relationships between the one-hole and two-hole ionization energies is to plot the modified two-hole ionization energies against the sum of the one-hole ionization energies. On such a plot, energies that involve the same values of R_{ij} will fall on a line with a slope of 1 and an intercept equal to $-R_{ij}$. Moreover, if one includes a line of slope 1 and 0 intercept, then points that involve positive values of R_{ij} will fall to one side of this line, and those with negative R_{ij} will fall to the other. This plot thus provides a simple way to visually summarize the relationships between these quantities.

Although the type of plot just described is useful, it does not relate easily to the traditional Wagner plot. One can, however, bring these two ideas together by subtracting the average one-hole ionization energy, $(I_{1,i} + I_{1,j})/2$, from both sides of eq 13, to give

$$I_{2,ij}^* - (I_{1,i} + I_{1,j})/2 = (I_{1,i} + I_{1,j})/2 - R_{ij} \dots \quad (14)$$

The left-hand side of this equation can be viewed as an average second core-hole ionization energy (modified by correcting for V_{ij}), which, accordingly, corresponds to the quantity that is plotted on the ordinate of a Wagner plot. Similarly, the first part of the right-hand side corresponds to the average first core-ionization energy. Thus, if one plots the quantity on the left versus $(I_{1,i} + I_{1,j})/2$, one has what could be regarded as a generalized Wagner plot that includes the two-site information. As was the case above, points that involve the same value of R_{ij}

fall on a line of unit slope and intercept equal to $-R_{ij}$. For the special case of $i = j$, corresponding to both holes being on the same site, this plot is identical to the traditional Wagner plot.

Figure 3 shows a generalized Wagner plot for the two-site ionization of uracil with one electron coming from one of the

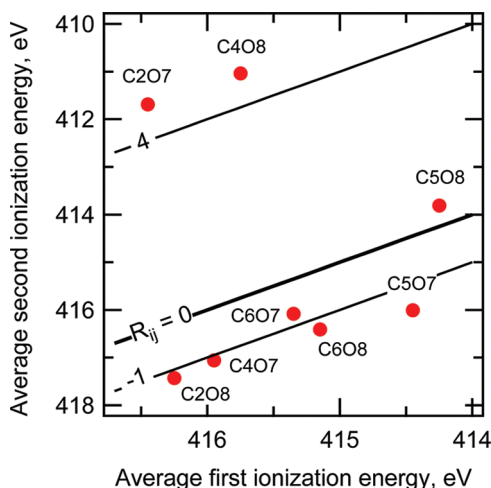
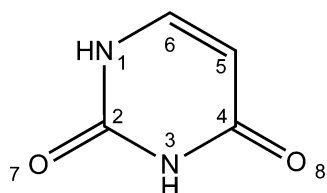


Figure 3. Generalized Wagner plot for two-site core ionization of uracil. Data are from Takahashi et al.¹² The black lines show loci of constant R_{ij} .

oxygen 1s cores and the other from one of the carbon 1s cores. The data for this plot were taken from Takahashi et al.¹² The numbering of the atoms in uracil is the same as was used by them and is illustrated in Scheme 1. In Figure 3, the general

Scheme 1. Uracil



systematics of the interatomic generalized relaxation energies, R_{ij} , are readily apparent. The points for C2O7 and C4O8 lie well above the line corresponding to $R_{ij} = 0$. The two holes that are created in these ionizations are close together, and the two positive charges work cooperatively to increase the overall relaxation above what it is for single-hole ionization. By contrast, C5 and O7 lie on opposite sides of the molecule, and consequently, they are competitive in their polarization, with each hole tending to undo the polarization caused by the other. As a result, the C5O7 point falls to the negative side of $R_{ij} = 0$. A similar but less pronounced situation applies to C2O8, C4O7, C6O7, and C6O8, all of which show values of $R_{ij} \approx -1$. Inspection of Scheme 1 shows that each of these pairs involves an ionized oxygen atom that is meta to the ionized carbon atom. The smallest deviation from $R_{ij} = 0$ is seen for C5O8, in which the ionized oxygen is ortho to the ionized carbon. In this case, the two holes are both competing and cooperating in the polarization of the molecule, with the cooperative effect being slightly greater than the competitive effect. Overall, one can see the not-surprising result that $R_{ij}(\text{ipso}) > R_{ij}(\text{ortho}) > 0 > R_{ij}(\text{meta}) > R_{ij}(\text{para})$. These ideas were discussed in some detail by Takahashi et al.¹² and are recapitulated here to illustrate how

the generalized Wagner plot provides a convenient way to visualize the results.

HIGHER-ORDER EFFECTS

Although there is qualitative agreement between the experimentally derived results and those presented here, there are noticeable disagreements in the details. The results presented in Table 1 show reasonable agreement between experiment and theory for the shifts in ionization energy but systematic disagreement between the values of ΔV and ΔR from the two different methods. In particular, the methods outlined here give values of ΔV and ΔR that are more positive than those derived from the experimental data. To resolve these apparent discrepancies, consider the higher-order terms that were omitted from eq 1.

Using the equivalent-cores approximation, one can evaluate the higher-order terms by considering, for example, the series of molecules BH_4^- , CH_4 , NH_4^+ , OH_4^{2+} , and FH_4^{3+} , which show the effects of the addition of a negative charge to the core or the addition of one, two, and three positive charges to the core, respectively. One can compare these with similar calculations for CF_4 , CCl_4 , and $\text{C}(\text{CH}_3)_4$ to assess the effects of the substituents relative to that of hydrogen. The results of these calculations are summarized in Figure 4, where the energies, $\Delta E(q)$, for $\text{CX}_4(q)$ relative to those of $\text{CH}_4(q)$ are plotted against q . [To simplify the presentation, the quantity plotted is $\Delta E(q) - \Delta E(0)$.] The data were fitted with two different polynomials. Shown in red are the fits for quartic polynomials to all five of the points. In blue are fits of quadratic polynomials to the points for $q = 0, 1$, and 2. Thus, the blue curves represent the results obtained when one omits the higher-order terms in eq 1.

In Figure 4, the vertical distances between the energies at $q = 0$ and the energies at $q = 1$ are the relative ionization energies, $\Delta I_1(0)$. The slopes of the curves at $q = 0$ are equal to ΔV , and the differences between these two quantities, $\Delta V - \Delta I_1(0)$, are equal to ΔR . One can see in this figure that the slopes of the quadratic fits, which ignore the higher-order terms, are, in every case, greater than the slopes obtained from the fits that include the higher-order terms. Thus, the model that was used in the preceding sections overestimates the values of ΔV . In addition, because the calculations give nearly correct values of $\Delta I_1(0)$, it also overestimates the values of ΔR . Qualitatively, at least, the error that arises from ignoring the higher-order terms is in the right direction to account for the discrepancies between the theoretically calculated values in Table 1 and the values based on experimental measurements.

To obtain a more quantitative picture of the comparison, it is necessary to be clear on how the quantity $(dE/dq)_0 \equiv V$ relates to a property of the neutral molecule. For removal of a proton from a molecule, this quantity can be identified rigorously with the potential energy of the proton.²² For removal of a core electron, it has been identified as the Koopmans-theorem energy, $-\epsilon$.^{17,18,29} In terms of the shift in energy between one molecular environment and another, one obtains

$$\left(\frac{d\Delta E}{dq} \right)_0 = -\Delta\epsilon = -\Delta V_e \quad (15)$$

where V_e is the potential energy of a core electron.⁴² For a core electron, the approximation that $-\Delta V_e = \Delta V_N$ has been widely used (where V_N is the potential energy of a positive charge at the nucleus of the atom). Both the orbital energy and the

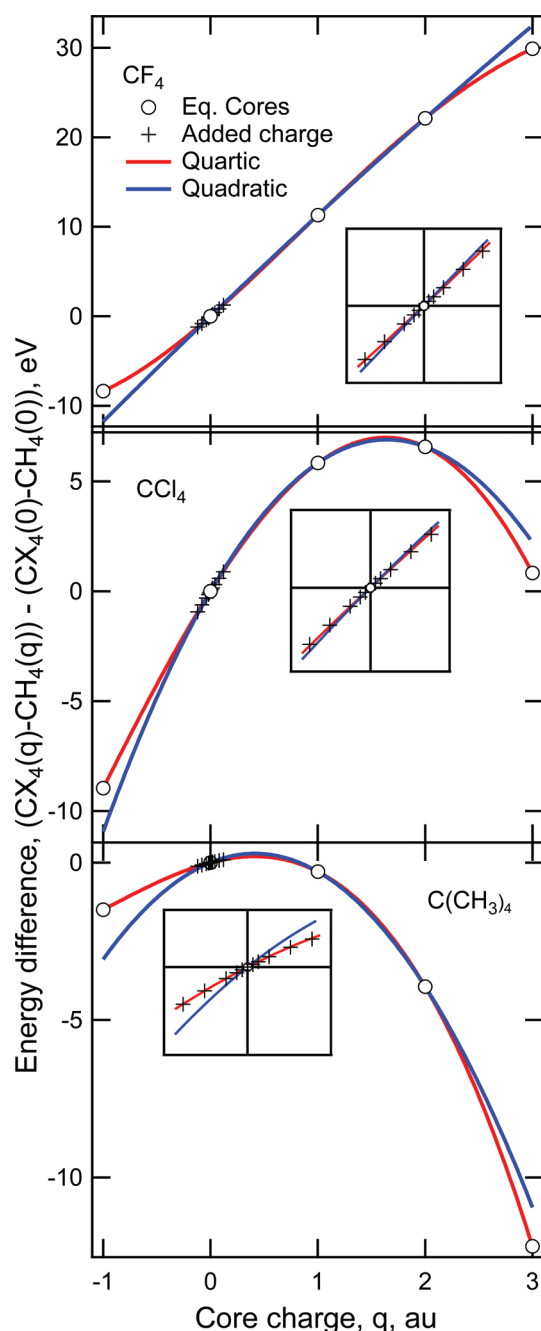


Figure 4. Energies of CX_4 relative to CH_4 as a function of excess charge, q , in the core of the central carbon atom. Open circles were calculated by the equivalent-cores method. Crosses show results obtained by adding small charges near the carbon center. The insets show an expanded view in the region of $q = 0$. The red lines show the fit of a quartic polynomial to all of the equivalent-cores result. The blue lines show the fit of a quadratic polynomial to the points with $q = 0, 1, 2$.

potential at the nucleus are easily calculated, and both have been widely used to estimate the initial-state effect on the core-ionization energy. However, the Koopmans-theorem energy has the disadvantage that it does not include correlation effects, and therefore, such effects have to be included as part of a generalized relaxation energy.¹¹ On the other hand, the use of ΔV_N does not take into account either the penetration of the valence wave functions into the core or any affect that changes in the valence wave functions might have on the core

electrons.³⁶ To get around these problems, Børve and Thomas³⁶ developed an “extended Koopmans theorem”. In its complete form, this approach is not convenient for general use, but a good approximation to it can be obtained with the expression

$$\Delta V_{\text{EKT}} = -\Delta\epsilon + (\Delta U_{\text{VCI}} - \Delta U_{\text{HF}}) \quad (16)$$

where V_{EKT} is the effect of the initial-state charge distribution on the core-ionization energy and ϵ is the orbital energy from a Hartree–Fock calculation. U_{VCI} and U_{HF} are the potential energies of a unit positive charge at the nucleus, the first being calculated using a valence-correlated wave function and the second using the Hartree–Fock method. Thus, the term in parentheses in eq 16 represent a correlation correction to the orbital energy. Although the differences among these terms are sometimes small, they are not negligible. For instance, for the comparison between 2,2-dimethylpropane and methane $\Delta V_{\text{EKT}} = 0.916$ eV, $-\Delta\epsilon = 0.699$ eV, $\Delta U_{\text{VCI}} = 1.025$ eV, and $\Delta U_{\text{HF}} = 0.807$ eV. The experimental values for ΔV listed in Table 1 were calculated with eq 16 using the MP2 method to obtain the valence-correlated potential energies. The values of ΔR were then obtained from the experimental ionization energies through the relationship $\Delta R = \Delta V - \Delta I_1(0)$.⁴³

One can see in Table 1 that the values of ΔV derived from using the first and second core-ionization energies are greater than those obtained from the use of the extended Koopmans theorem. In Figure 4, one can see that the slopes of the curves at $q = 0$ (which are equal to ΔV) are greater for the three-point fits than the fits to all five points. The appropriate question is then “Do the slopes from the five-point fits agree with the values from the extended Koopmans theorem?” A comparison of the different results is shown in Table 2, where one can see

Table 2. Values of the Initial Contribution, ΔV , to the Shift in Ionization Energy between CX_4 and CH_4

	EKT	equivalent cores	added charge
CF_4	10.022	10.468	10.240
CCl_4	7.343	7.782	7.554
$C(CH_3)_4$	0.916	0.895	0.886

that there is reasonably good agreement between the values derived from the wave functions of the neutral molecule (the extended Koopmans-theorem values) and those derived from varying the core charge in the molecule (crosses in Figure 4). Thus, it appears that the extended Koopmans theorem of Børve and Thomas provides an accurate method of estimating the initial-state effect and that combining this estimate with experimental ionization energies provides an accurate measurement of the effect of relaxation on the ionization energy. By contrast, the use of the first and second core-hole ionization energies, although it gives results that are qualitatively correct, leads (in the cases investigated here) to an overestimate of both the initial-state effect and the relaxation.

The results reported by Tashiro et al.¹¹ also show that the values of ΔV derived from using the first and second core-ionization energies are different from those obtained using Koopmans theorem and the first core-ionization energy. For a number of systems, they showed that the relaxation energy associated with double core ionization is approximately 4 times that for single ionization, as expected from eqs 3 and 6. However, in detail, there are systematic deviations from this value. In particular, their calculations show values slightly

greater than 4 for ethane, ethene, and ethyne but slightly less than 4 for carbon monoxide and carbon dioxide. Although these differences appear to be relatively minor when one considers the total relaxation energies, they become significant when one considers the differences in relaxation energy between two different compounds, such as ethane and carbon dioxide. Using the difference between the Koopmans-theorem energy and the calculated ionization energy, Tashiro et al. found relaxation energies of 13.89 and 14.28 eV, respectively, leading to a difference in relaxation energies of 1.14 eV. From comparing the calculated one-hole and two-hole ionization energies, they obtained values for the relaxation energies of 11.87 and 15.06 eV, for a difference of 3.19 eV. The two methods agree that the relaxation associated with ethane is greater than that associated with carbon monoxide, but they disagree significantly on the actual difference.⁴⁴

DISCUSSION AND CONCLUSIONS

Evaluating the effects of the initial-state charge distribution and the final-state charge rearrangement on the energies for such chemical processes as ionization, protonation, and deprotonation is important for obtaining a better understanding of these phenomena. Comparison of one-hole ionization energies with single-site two-hole ionization energies provides one of the few fully experimental methods for determining the relative importance of these two effects. As a result, there has been, over a long period of time, considerable interest in measuring these ionization energies. Until recently, however, measuring the two-hole ionization energies has relied on core–core–core Auger spectroscopy, which is limited to elements beyond the first row of the periodic table. The recent demonstrations that two-hole ionization energies can be measured directly in first-row elements opens up a wealth of opportunities.

The equations that are used to determine values of ΔV and ΔR omit the higher-order terms in eq 1. Analysis of the effect of these terms indicates that the values of ΔV and ΔR determined from comparison of one- and two-hole ionization energies will differ quantitatively from those determined by other techniques, but that the differences are small in magnitude.

Recent discussions have often emphasized that the chemical shifts of the two-hole ionization energies are significantly greater than those for the one-hole ionization energies. This result can be seen by comparing eqs 3 and 6, where one can see that the chemical shift for the two-hole ionization energy can be 2–4 times that for the one-hole ionization energy, depending on the relative importance of ΔV and ΔR . However, this is not the most important difference between the two ionization energies, partially because, with current techniques, it is difficult to exploit the larger shifts associated with two-hole ionization. At present, it is possible to measure carbon 1s core-ionization energy shifts with uncertainties of between 0.01 and 0.02 eV,³² but the uncertainties reported for carbon 1s two-hole ionization energies range from 0.5^{7,9} to 3.5⁸ eV.

Although one might expect improvements in the accuracy with which the two-hole ionization energies can be determined, the significant point is not that the shifts are greater for the two-hole ionization energies, but rather that they provide *different* information from that available from the one-hole ionization energies. This difference is apparent from eqs 3 and 6, and it is this difference that is the basis for determining ΔV and ΔR , as has been discussed above. Even if the shifts in two-hole ionization energies are equal to those for the one-hole ionization energies, as is the case for the carbon 1s ionization

energies in uracil,¹² this is important information, namely, that the relaxation energy is the same for all of these carbon atoms.

Recently, it has been demonstrated that it is possible to measure two-site double-hole ionization energies,^{8,9} and a number of authors have suggested that these values will be a source of new information of chemical interest.^{10–12} It is not yet clear, however, what this new information is and how it can be related to questions that are chemically interesting. From eq 11, one can see that these energies differ from the one-hole ionization energies by the quantities $V_{ij} = 1/r_{ij}$ and R_{ij} . Both of these quantities vary in a systematic way with the positions of the two atoms in the molecule.

A possible application of two-site double-hole ionization can be illustrated by considering *n*-butane, CH₃CH₂CH₂CH₃. This molecule exists in two conformers, anti and gauche, and both are present at room temperature.⁴⁵ Calculations of the sort described above using the B3LYP method and the triple- ζ basis set show that there is very little difference between the two conformers for the one-hole and single-site two-hole ionization energies. For the two-site double-hole ionization energies, there are no significant differences except for the C1C4 ionization, where the difference is calculated to be 0.27 eV, with gauche greater than anti. In the anti form, the distance between the two terminal carbons, C1 and C4, is 3.900 Å, whereas for the gauche form, it is 3.072 Å; all of the other interatomic distances are essentially independent of the conformation.⁴⁵ Thus, the difference in V_{14} is 1.0 eV. This is partially offset by the contribution from R_{14} (competitive for the anti form and cooperative for the gauche form) to give the predicted overall value for ΔI_2 of 0.27 eV. Although this value is small compared with the presently available resolution for this kind of experiment, there is the possibility that, with improved resolution, two-site double-hole ionization could be used as a tool for conformational studies.

The fragmentation of *n*-butane following ionization provides a possible target for investigation by (PE)²(PI)⁺CO spectroscopy.⁴⁶ For single ionization of a core electron, the fragmentation into ions occurs after an Auger deexcitation and is largely determined by the properties of the molecular ion having two holes in the valence shell. As a result, there is decoupling between the fragmentation pattern and the site of initial ionization. By contrast, for double core ionization there is, in some cases, the possibility that fragmentation will precede Auger decay and that the fragmentation pattern might be very specific to the site of ionization. For instance, the calculations show that, for ionization of *n*-butane at C1, there will be dissociation into C²⁺H₃⁺ and CH₂CH₂CH₃⁺, where the double asterisk indicates that there are two carbon 1s holes on this fragment. Except for possible vibrational excitation, the propyl cation is stable and will be detected as such. The methyl fragment decays by a double Auger process, leading to such species as H⁺, H₂⁺, C²⁺, and CH⁺. By contrast, double ionization at C2 will lead to dissociation into CH₃C²⁺H₂⁺ and CH₂CH₃⁺. The ethyl group that has no core hole will be detected as such, whereas the group with two core holes will decay by double Auger decay to CH₃CH₂³⁺, which will then decay to a variety of fragments. Thus, the fragmentation patterns for the two different kinds of ionization can be expected to be quite different.

In general, our expectation is that a doubly ionized molecule will fragment rapidly because of the strong Coulomb repulsion associated with the positive charges. Surprisingly, this is not necessarily the case for double core ionization. For instance, the

calculations described here show that the ions $C^{*}X_4^{2+}$ ($X = H, F, CH_3$) have metastable tetrahedral configurations, with CX bond lengths not much different from those of the neutral molecule. Calculations by Boldyrev and Simons⁴⁷ on OH_4^{2+} , which is the ion with a core equivalent to that of doubly core-ionized methane, show that, although the ion is unstable by about 3 eV with respect to dissociation into OH_3^+ and H^+ , there is a barrier of almost 2 eV against this dissociation. As was discussed by Boldyrev and Simons, this metastability arises because the charge can be delocalized over the symmetric molecule. A similar situation exists for double core ionization of 1,3-butadiene, $CH_2CHCHCH_2$, where resonance allows the charge to be delocalized over the entire molecule. Thus, double core ionization at either C1 or C2 in 1,3-butadiene leads to a metastable species, in contrast to the situation for *n*-butane, where the same ionizations lead to dissociative species.

In summary, it appears that the newly developing ability to measure double-hole core-ionization energies in such elements as carbon, nitrogen, and oxygen opens up interesting possibilities for providing new insights into initial-state and final-state effects in chemical processes that involve charge addition to a molecule. The Wagner plot provides a convenient way to display these energies and their relationships, and it can be generalized to include two-site double core ionization. Appropriate attention needs to be paid to the higher-order effects on these energies, but it appears that these do not change the qualitative conclusions that can be drawn from comparison of single-hole and double-hole energies. In addition, there is the possibility that studies of double-hole ionization can provide information on molecular conformation, on the metastability of doubly ionized species, and on the fragmentation of such species.

AUTHOR INFORMATION

Corresponding Author

*E-mail: t.darrah.thomas@oregonstate.edu.

Notes

The authors declare no competing financial interest.

ACKNOWLEDGMENTS

I am indebted to Knut Børve for helpful suggestions with regard to the theoretical calculations.

REFERENCES

- (1) (a) Kowalczyk, S. P.; Pollak, R. A.; McFeely, F. R.; Ley, L.; Shirley, D. A. *Phys. Rev. B* **1973**, *8*, 2387–2391. (b) Kowalczyk, S. P.; Ley, L.; McFeely, F. R.; Pollak, R. A.; Shirley, D. A. *Phys. Rev. B* **1974**, *9*, 381–391. (c) Bahl, M. K.; Woodall, R. O.; Watson, R. L.; Irgolic, K. J. *J. Chem. Phys.* **1976**, *64*, 1210–1218. (d) Bahl, M. K.; Watson, R. L.; Irgolic, K. J. *J. Chem. Phys.* **1978**, *68*, 3272–3279. (e) Franke, R.; Chassé, T.; Streubel, P.; Meisel, A. *J. Electron Spectrosc. Relat. Phenom.* **1991**, *56*, 381–388. (f) Wong, J.; Sun, W.; Ma, Z.; Sou, I. *J. Electron Spectrosc. Relat. Phenom.* **2001**, *113*, 215–220. (g) Eickhof, T.; Medicherla, V.; Drube, W. *J. Electron Spectrosc. Relat. Phenom.* **2004**, *137–140*, 85–88.
- (2) Gaarenstroom, S. W.; Winograd, N. *J. Chem. Phys.* **1977**, *67*, 3500–3506.
- (3) (a) Ashe, A. J., III; Bahl, M. K.; Bomben, K. D.; Chan, W. T.; Gimzewski, J. K.; Sittion, P. G.; Thomas, T. D. *J. Am. Chem. Soc.* **1979**, *101*, 1764–1767. (b) Aitken, E. J.; Bahl, M. K.; Bomben, K. D.; Gimzewski, J. K.; Nolan, G. S.; Thomas, T. D. *J. Am. Chem. Soc.* **1980**, *102*, 4873–4879. (c) Sæthre, L. J.; Thomas, T. D. *J. Org. Chem.* **1991**, *56*, 3935–3942.
- (4) (a) Nolan, G. S.; Sæthre, L. J.; Siggel, M. R.; Thomas, T. D.; Ungier, L. *J. Am. Chem. Soc.* **1985**, *107*, 6463–6467. (b) Siggel, M. R. F.; Nolan, G. S.; Sæthre, L. J.; Thomas, T. D.; Ungier, L. *J. Phys. Chem.* **1987**, *91*, 3969–3974.
- (5) (a) Sodhi, R. N.; Cavell, R. G. *J. Electron Spectrosc. Relat. Phenom.* **1983**, *32*, 283–312. (b) Sodhi, R. N. S.; Cavell, R. G. *J. Electron Spectrosc. Relat. Phenom.* **1986**, *41*, 1–24. (c) Cavell, R. G.; Sodhi, R. N. *J. Electron Spectrosc. Relat. Phenom.* **1986**, *41*, 25–36.
- (6) (a) Young, L.; Kanter, E. P.; Krässig, B.; Li, Y.; March, A. M.; Pratt, S. T.; Santra, R.; Southworth, S. H.; Rohringer, N.; DiMauro, L. F.; Doumy, G.; Roedig, C. A.; Berrah, N.; Fang, L.; Hoener, M.; Bucksbaum, P. H.; Cryan, J. P.; Ghimire, S.; Glowina, J. M.; Reis, D. A.; Bozek, J. D.; Bostedt, C.; Messerschmidt, M. *Nature* **2010**, *466*, 56–61. (b) Cryan, J. P.; Glowina, J. M.; Andreasson, J.; Belkacem, A.; Berrah, N.; Blaga, C. I.; Bostedt, C.; Bozek, J.; Buth, C.; DiMauro, L. F.; Fang, L.; Gessner, O.; Guehr, M.; Hajdu, J.; Hertlein, M. P.; Hoener, M.; Kornilov, O.; Marangos, J. P.; March, A. M.; McFarland, B. K.; Merdji, H.; Petrović, V. S.; Raman, C.; Ray, D.; Reis, D.; Tarantelli, F.; Trigo, M.; White, J. L.; White, W.; Young, L.; Bucksbaum, P. H.; Coffee, R. N. *Phys. Rev. Lett.* **2010**, *105*, 083004. (c) Fang, L.; Hoener, M.; Gessner, O.; Tarantelli, F.; Pratt, S. T.; Kornilov, O.; Buth, C.; Gühr, M.; Kanter, E. P.; Bostedt, C.; Bozek, J. D.; Bucksbaum, P. H.; Chen, M.; Coffee, R.; Cryan, J.; Glowina, M.; Kuk, E.; Leone, S. R.; Berrah, N. *Phys. Rev. Lett.* **2010**, *105*, 083005. (d) Linusson, P.; Takahashi, O.; Ueda, K.; Eland, J. H. D.; Feifel, R. *Phys. Rev. A* **2011**, *83*, 022506. (e) Lablanquie, P.; Penent, F.; Palaudoux, J.; Andric, L.; Selles, P.; Carniato, S.; Bucar, K.; Žitnik, M.; Huttula, M.; Eland, J. H. D.; Shigemasa, E.; Soejima, K.; Hikosaka, Y.; Suzuki, I. H.; Nakano, M.; Ito, K. *Phys. Rev. Lett.* **2011**, *106*, 063003.
- (7) Eland, J. H. D.; Tashiro, M.; Linusson, P.; Ehara, M.; Ueda, K.; Feifel, R. *Phys. Rev. Lett.* **2010**, *105*, 213005.
- (8) Berrah, N.; Fang, L.; Murphy, B.; Osipov, T.; Ueda, K.; Kuk, E.; Feifel, R.; van der Meulen, P.; Salen, P.; Schmidt, H. T.; Thomas, R. D.; Larsson, M.; Richter, R.; Prince, K. C.; Bozek, J. D.; Bostedt, C.; Wada, S.; Piancastelli, M. N.; Tashiro, M.; Ehara, M. *Proc. Natl. Acad. Sci. U.S.A.* **2011**, *108*, 16912–16915.
- (9) Lablanquie, P.; Grozdanov, T. P.; Žitnik, M.; Carniato, S.; Selles, P.; Andric, L.; Palaudoux, J.; Penent, F.; Iwayama, H.; Shigemasa, E.; Hikosaka, Y.; Soejima, K.; Nakano, M.; Suzuki, I. H.; Ito, K. *Phys. Rev. Lett.* **2011**, *107*, 193004.
- (10) (a) Cederbaum, L. S.; Tarantelli, F.; Sgamellotti, A.; Schirmer, J. *J. Chem. Phys.* **1986**, *85*, 6513–6523. (b) Cederbaum, L. S.; Tarantelli, F.; Sgamellotti, A.; Schirmer, J. *J. Chem. Phys.* **1987**, *86*, 2168–2175. (c) Santra, R.; Kryzhevoi, N. V.; Cederbaum, L. S. *Phys. Rev. Lett.* **2009**, *103*, 013002. (d) Kryzhevoi, N. V.; Santra, R.; Cederbaum, L. S. *J. Chem. Phys.* **2011**, *135*, 084302.
- (11) Tashiro, M.; Ehara, M.; Fukuzawa, H.; Ueda, K.; Buth, C.; Kryzhevoi, N. V.; Cederbaum, L. S. *J. Chem. Phys.* **2010**, *132*, 184302.
- (12) Takahashi, O.; Tashiro, M.; Ehara, M.; Yamasaki, K.; Ueda, K. *J. Phys. Chem. A* **2011**, *115*, 12070–12082.
- (13) Takahashi, O.; Tashiro, M.; Ehara, M.; Yamasaki, K.; Ueda, K. *Chem. Phys.* **2011**, *384*, 28–35.
- (14) Liberman, D. *Bull. Am. Phys. Soc.* **1964**, *9*, 731.
- (15) Hedin, L.; Johansson, A. *J. Phys. B* **1969**, *2*, 1336–1346.
- (16) (a) Wagner, C. D. *Anal. Chem.* **1975**, *47*, 1201–1203. (b) Wagner, C. D. *Faraday Discuss. Chem. Soc.* **1975**, *60*, 291–300.
- (17) Williams, A. R.; Lang, J. D. *Phys. Rev. Lett.* **1978**, *40*, 954–957.
- (18) Thomas, T. D. *J. Electron Spectrosc. Relat. Phenom.* **1980**, *20*, 117–125.
- (19) Martin, R. L.; Shirley, D. A. *J. Am. Chem. Soc.* **1974**, *96*, 5299–5304.
- (20) Davis, D. W.; Shirley, D. A. *J. Am. Chem. Soc.* **1976**, *98*, 7898–7903.
- (21) (a) Smith, S. R.; Thomas, T. D. *J. Am. Chem. Soc.* **1978**, *100*, 5459–5466. (b) Siggel, M. R.; Thomas, T. D. *J. Am. Chem. Soc.* **1986**, *108*, 4360–4363. (c) Siggel, M. R. F.; Thomas, T. D. *J. Am. Chem. Soc.* **1992**, *114*, 5795–800.
- (22) Ji, D.; Thomas, T. D. *J. Phys. Chem.* **1994**, *98*, 4301–4303.

- (23) Davis, D. W.; Rabalais, J. W. *J. Am. Chem. Soc.* **1974**, *96*, 5305–5310.
- (24) Mills, B. E.; Martin, R. L.; Shirley, D. A. *J. Am. Chem. Soc.* **1976**, *98*, 2380–2385.
- (25) (a) Benoit, F. M.; Harrison, A. G. *J. Am. Chem. Soc.* **1977**, *99*, 3980–3984. (b) Cavell, R. G.; Allison, D. A. *J. Am. Chem. Soc.* **1977**, *99*, 4203–4204. (c) Brown, R. S.; Tse, A. J. *Am. Chem. Soc.* **1980**, *102*, 5222–5226. (d) Nordfors, D.; Mårtensson, N.; Ågren, H. *J. Electron Spectrosc. Relat. Phenom.* **1990**, *53*, 129–139. (e) Nordfors, D.; Mårtensson, N.; Ågren, H. *J. Electron Spectrosc. Relat. Phenom.* **1991**, *56*, 167–187. (f) Carroll, T. X.; Thomas, T. D.; Bergersen, H.; Børve, K. J.; Sæthre, L. J. *J. Org. Chem.* **2006**, *71*, 1961–1968. (g) Carroll, T. X.; Thomas, T. D.; Sæthre, L. J.; Børve, K. J. *J. Phys. Chem. A* **2009**, *113*, 3481–3490.
- (26) Myrseth, V.; Sæthre, L. J.; Børve, K. J.; Thomas, T. D. *J. Org. Chem.* **2007**, *72*, 5715–5723.
- (27) (a) Sæthre, L. J.; Thomas, T. D.; Svensson, S. *J. Chem. Soc., Perkin Trans. 2* **1997**, 749–755. (b) Thomas, T. D.; Sæthre, L. J.; Børve, K. J.; Gundersen, M.; Kuk, E. *J. Phys. Chem.* **2005**, *109*, 5085.
- (28) Equation 1 applies only to single-site ionization. Equation 10 provides a general expression for two-site ionization.
- (29) Janak, J. F. *Phys. Rev. B* **1978**, *18*, 7165–7168.
- (30) Results from Tashiro et al.¹¹ indicate that V_C might depend slightly on the molecular composition. This question needs further investigation.
- (31) Frisch, M. J.; Trucks, G. W.; Schlegel, H. B.; Scuseria, G. E.; Robb, M. A.; Cheeseman, J. R.; Scalmani, G.; Barone, V.; Mennucci, B.; Petersson, G. A.; Nakatsuji, H.; Caricato, M.; Li, X.; Hratchian, H. P.; Izmaylov, A. F.; Bloino, J.; Zheng, G.; Sonnenberg, J. L.; Hada, M.; Ehara, M.; Toyota, K.; Fukuda, R.; Hasegawa, J.; Ishida, M.; Nakajima, T.; Honda, Y.; Kitao, O.; Nakai, H.; Vreven, T.; Montgomery, J. A., Jr.; Peralta, J. E.; Ogliaro, F.; Bearpark, M.; Heyd, J. J.; Brothers, E.; Kudin, K. N.; Staroverov, V. N.; Kobayashi, R.; Normand, J.; Raghavachari, K.; Rendell, A.; Burant, J. C.; Iyengar, S. S.; Tomasi, J.; Cossi, M.; Rega, N.; Millam, J. M.; Klene, M.; Knox, J. E.; Cross, J. B.; Bakken, V.; Adamo, C.; Jaramillo, J.; Gomperts, R. E.; Stratmann, O.; Yazyev, A. J.; Austin, R.; Cammi, C.; Pomelli, J. W.; Ochterski, R.; Martin, R. L.; Morokuma, K.; Zakrzewski, V. G.; Voth, G. A.; Salvador, P.; Dannenberg, J. J.; Dapprich, S.; Daniels, A. D.; Farkas, O.; Foresman, J. B.; Ortiz, J. V.; Cioslowski, J.; Fox, D. J. *Gaussian 09*, revision A.1; Gaussian Inc.: Wallingford, CT, 2009.
- (32) Holme, A.; Børve, K. J.; Sæthre, L. J.; Thomas, T. D. *J. Chem. Theory Comput.* **2011**, *7*, 4104–4114.
- (33) (a) Thomas, T. D.; Sæthre, L. J.; Børve, K. J.; Bozek, J. D.; Huttula, M.; Kuk, E. *J. Phys. Chem. A* **2004**, *108*, 4983–4990. (b) Sæthre, L. J.; Børve, K. J.; Thomas, T. D. *J. Electron Spectrosc. Relat. Phenom.* **2011**, *183*, 2–9.
- (34) The values of ΔR derived from the experimental results are actually part experimental and part theoretical, being the difference between the measured shifts in ionization energy and values of ΔV calculated from the properties of the neutral molecules.
- (35) Calculations by Takahashi et al.¹³ on SiX_4 are in accord with these results for $X = \text{F}$ and $X = \text{Cl}$ (relative to $X = \text{H}$), showing that the shift due to replacing hydrogen with fluorine primarily results from the initial-state effect, with little contribution from relaxation, whereas the shift due to chlorine results from a large initial-state effect that is partially offset by relaxation. Their results for $\text{Si}(\text{CH}_3)_4$ indicate a negative initial-state effect for the methyl group, in contrast to the results seen here for $\text{C}(\text{CH}_3)_4$, for which the initial-state effect is positive.
- (36) Børve, K. J.; Thomas, T. D. *J. Electron Spectrosc. Relat. Phenom.* **2000**, *107*, 155–161.
- (37) Moretti, G. *J. Electron Spectrosc. Relat. Phenom.* **1998**, *95*, 95–144.
- (38) Wagner, C. D. *J. Electron Spectrosc. Relat. Phenom.* **1977**, *10*, 305–315.
- (39) NIST X-ray Photoelectron Spectroscopy Database, version 3.5; NIST Standard Reference Database 20; National Institute of Standards and Technology, Gaithersburg, 2003. Wagner plots available at <http://srdata.nist.gov/xps/WagnerPlot.aspx> (accessed April 2012).
- (40) This is not strictly true. For instance, Sodhi and Cavell⁵ observed that the shifts in the sulfur and phosphorus 2p ionization energies in a variety of compounds are only 86% of the shifts in the 1s ionization energies.
- (41) (a) Myrseth, V.; Bozek, J. D.; Kuk, E.; Sæthre, L. J.; Thomas, T. D. *J. Electron Spectrosc. Relat. Phenom.* **2002**, *122*, 57. (b) Feyer, V.; Plekan, O.; Richter, R.; Coreno, M.; Vall-lloera, G.; Prince, K. C.; Trofimov, A. B.; Zaytseva, I. L.; Moskovskaya, T. E.; Gromov, E. V.; Schirmer, J. *J. Phys. Chem. A* **2009**, *113*, 5736–5742.
- (42) Schwartz, M. E. *Chem. Phys. Lett.* **1970**, *6*, 631–535.
- (43) The rationale for using the experimental ionization energy rather than a theoretically calculated ionization energy is that the relative experimental ionization energies are known with an accuracy of 0.01–0.02 eV, whereas theoretically calculated ionization energies, which involve simulation of a core hole, can be quite uncertain. With the approach used here, the derived values of ΔR thus depend only on an accurately known ionization energy and calculated properties of the neutral molecule.
- (44) In addition to the effects of the higher-order terms in eq 1 the results reported in ref 11 are affected by correlation effects, which are larger for carbon monoxide than for ethane and for differences between the Coulomb interaction energy of the two core holes in the different molecules.
- (45) Bonham, R. A.; Bartell, L. S. *J. Am. Chem. Soc.* **1959**, *81*, 3491–3496.
- (46) Two photoelectrons in coincidence with n ions.
- (47) Boldyrev, A. I.; Simons, J. *J. Chem. Phys.* **1992**, *97*, 4272–4281.